# BUBBLE SIZE DISTRIBUTION OF FOAM

**C.W. den Engelsen[a], J.C. Isarin[b], H. Gooijer[a], M.M.C.G. Warmoeskerken[c] and J. Groot Wassink[c]**

[a] Stork Brabant BV
W. de Korverstraat 43
5831 AN Boxmeer
The Netherlands

[b] TNO
M.H. Tromplaan 28
7513 AB Enschede
The Netherlands

[c] Textile Research Group
Department of Chemical Technology
University of Twente
P.O. Box 217
7500 AE Enschede,
The Netherlands

E-mail: marijn.warmoeskerken@unilever.com

## *Abstract*

*A procedure based upon image analysis has been adopted to study the influence of several physical parameters on bubble size in foam. A procedure has been described to account for the distribution of bubble size. Foam was generated in a rotor-stator mixer. In the present research, the nature of the surfactant, liquid viscosity, solid phase content, and rotational speed of the mixer were varied. All parameters were found to influence the bubble size and its distribution to a certain extent. These effects were qualified experimentally.*

***Key words:*** *foam, bubble size, size distribution, image analysis*

## Introduction

Foams are the subject of practical interest in a number of major working fields, for instance, in the textile finishing industry. During the application of foam on textile substrates, bubble size is considered to be of major importance for the quality of the end-product, especially when colorants are involved [1]. Bubble size also has an impact on the foam application process through the rheological behaviour of foam [2,3] and foam stability [4,5]. The distribution probably has an even more pronounced influence on these aspects. Apart from the textile industry, foam finds interesting applications for fire-fighting purposes, in the food industry and in enhanced oil recovering [6].

Numerous studies have been made on determining the size of gas bubbles in foam, and on the related issue of liquid droplets in emulsions. Several experimental techniques have been applied in studying bubble size and its distribution. Bisperink *et al.* [7] presented a brief survey on earlier work on the subject. The authors also performed measurements with an apparatus which uses an optical glass fibre technique. They found volume surface-average bubble diameters within the range of ten to several hundred μm. This method was also applied to study disproportion.

Gido *et al.* [8] performed a study on the size of foam bubbles as a function of the rotational speed in a dynamic mixer. The authors found for two different foam densities that increasing the rotational speed of the mixer caused a decrease in the average bubble diameter. The average bubble diameter was slightly smaller for foam with the lower density. After the foam flowed through a porous medium, there was no

dependence of the rotational speed of the mixer on the bubble size. The size of the bubbles after exiting the porous medium was approximately equal to the size of the pores. No information has been given about the bubble size distribution.

A study on the size of bubbles in foam in a dynamic (rotor-stator) mixer has also been conducted by Kroezen [9]. The author found that the mean bubble diameter decreased with increasing rotational speed of the mixer. This was ascribed to an increase of the shear stress in the mixer at higher rotational speeds. A non-linear dependence was found for the distribution of the bubble sizes compared to the mean bubble size. The standard deviation was relatively larger for greater mean bubble sizes. A Newton-Reynolds relation was derived, with which it was possible to determine a laminar, a turbulent, and a transition flow field in the mixer. A decrease in the mean bubble diameter was found for increasing foam density. A shorter residence time in the mixer was found to increase the mean bubble diameter, especially for low-density foam.

Hirt *et al.* [10] studied the size of bubbles of high-density foam. The foam was generated in a dynamic mixer. An increase of the rotational speed of the mixer caused a decrease of the mean bubble size. An increase of the viscosity of the liquid phase resulted in a smaller mean bubble size. The measured bubble diameters were in the range of 150-800 μm when a liquid phase with a low viscosity was foamed. For a liquid phase with high viscosity, the measured bubble diameters were in the range of 60-465 μm. A non-linear empirical model was derived to predict the mean bubble diameter from the rotational speed of the mixer, the gas flow rate, and the liquid flow rate.

Isarin *et al.* [1] used an image analysis technique to determine the bubble size and its distribution of foam as generated in a dynamic mixer. The authors found mean bubble radii of 30-50 μm; the influences of rotational speed of the mixer and foam density were established. The technique was also adopted to monitor disproportion. The authors found good reproducibility in their results.

Chang *et al.* [11] determined the size of foam bubbles by freezing small samples, from which they determined the bubble size and the distribution. The authors showed that freezing did not alter the size of the bubbles. The bubble size distribution inside the sample of foam was almost the same as that on the outer surface. An increase of the expansion ratio caused a decrease of the average bubble size.

Calvert & Nezhati [12] performed a study on the bubble size distribution of foam generated in a static mixer. The mean bubble sizes were in the range of 120 μm to 220 μm, independent of the foam density.

Thondavadi & Lemlich [13] measured the bubble size of low density two- and three-phase foam in a study on the flow behaviour of foam in pipes. Foam was generated in a static mixer. The bubble diameters were found to be between 100 μm and 1000 μm. No influence was observed on the foam density, the bubble size, or the existence of solid particles on the flow behaviour of the foams.

De Vries [14] measured the radii of gas bubbles in foams generated of various liquid phases. A dynamic 'Household Whipping Apparatus' was used for generating the foams. Mean radii of 23-90 μm were found. The author derived a mathematical equation for the distribution of the radii of the gas bubbles in the various foams. De Vries found the model to fit satisfactorily to the experimental results, although the author admits that not all distributions can be described by one mathematical equation.

From these earlier studies, it can be concluded that only a few authors have researched the bubble size distribution quantitatively. Little is known about the influence of the liquid viscosity and the presence of solid particles on the bubble size distribution. In the present work, the influence of a solid phase on the bubble size and its distribution has been studied. Furthermore, the influence of the nature of the surface active agent has been studied, as well as the influence of the viscosity of the liquid phase. In all experiments the influence of the rotational speed of the mixer was an important parameter.

## Distribution

From the preceding section, it appears that foam bubble diameters have been found in the approximate range of 10 μm to 1 mm. An increase of the rotational speed of a dynamic mixer results in a smaller

mean bubble diameter. The bubble size is also affected by the viscosity of the liquid phase; a lower viscosity results into larger mean bubbles. Due to disproportion, small bubbles will shrink and large bubbles will grow. This phenomenon results in an increase of the distribu tion of the bubble size. Polydispersity and deviations from the ideal spherical bubble shape occur because of the large gas fraction in foam. It is striking in the literature that the mean values are mostly measured, and hardly any information is given about the distribution of the foam bubbles, whilst the distribution has a large impact on, for instance, foam stability.

To account for a distribution in the bubble radii, Isarin *et al.* [1] introduced a scattering in the average bubble radius, calculated in the same way as a standard deviation for a normal distribution. Standard deviations have been calculated more often in the literature [9]. But for abnormal distribu tion functions, a standard deviation is not a useful parameter to account for the distribution of the bubble size.

De Vries [14] presented an empirical obtained relation for the distribu tion of the bubble size, which can be expressed in dimensionless form by division through the average radius: $R = r / \bar{r}$

$$F(r) = \frac{2.082\,R}{\left(1 + 0.347\,R^2\right)^4} \tag{1}$$

Another relation for the distribution has been presented by Ranadive & Lemlich [5] in dimensionless form:

$$\mathrm{F}(r) = \frac{32}{\pi^2} R^2\, e^{-\frac{4}{\pi}R^2} \tag{2}$$

Gal-Or & Hoelscher [15] have derived a relation which is very similar to the Ranadive & Lemlich relation:

$$\mathrm{F(r)} = \frac{16}{\pi} R^2\, e^{-\left(\frac{16}{\pi}\right)^{\frac{1}{3}}R^2} \tag{3}$$

Also, gamma distributions [16] or log-normal distributions [17] have been used to describe the bubble size distribution in foam.

A few options are possible to calculate an average radius from an experiment which gives a series of radii. One is the number-average radius ($r_{10}$) defined by:

$$r_{10} = \frac{1}{n}\sum_{i=1}^{n} r_i \tag{4}$$

All radii attribute to the average value in the same magnitude. Another option to calculate is the volume-average bubble radius ($r_{30}$), defined by:

$$r_{30} = \left\{\frac{1}{n}\sum_{i=1}^{n} r_i^3\right\}^{\frac{1}{3}} \tag{5}$$

Large bubbles make a larger contribution to the volume-average bubble radius, hence, $r_{30} > r_{10}$. The volume-surface-average or Sauter bubble radius ($r_{32}$) is another way of accounting for a mean bubble radius:

$$r_{32} = \frac{\sum_{i=1}^{n} r_i^3}{\sum_{i=1}^{n} r_i^2} \tag{6}$$

Surface-average bubble radii could be calculated likewise. Each average radius has its own unique standard deviation.

Apart from average bubble radii, there are other values that may be important in a bubble size experiment [18]. The mode is the value which appears most frequently. The median is the value of which 50% of the radii are larger and 50% are smaller. For a normal distribution: mode = mean = median. A mode and median value in a volume distribution can differ from those values in a number distribution. A number that accounts for non-abnormality is the skewness number Sk [18]. Usually, skewness is made dimensionless by division through the variance to the power 3/2 :

$$Sk = \frac{\frac{1}{n}\sum_{i=1}^{n}\left(r_i - \bar{r}\right)^3}{\left\{\frac{1}{n-1}\sum_{i=1}^{n}\left(r_i - \bar{r}\right)^2\right\}^{\frac{3}{2}}} \qquad (7)$$

where $\bar{r}$ could be, for instance, $r_{10}$ or $r_{30}$. It is possible to calculate a skewness number for the volume distribution as well as for the number distribution. A distribution skewed to the right has a positive skewness number; a distribution skewed to the left has a negative skewness number [18]. A symmetrical distribution has a skewness number of zero.

Another way to account for the distribution of the bubble size is to calculate radii belonging to an interval of, *e.g.*, 40% smaller than the median value and 40% larger than the median value, either for a volume or a number distribution [6,19]. The scattering of a distribution is the value of this interval. The scattering of the number distribution is thus $r_{0.9*n}$-$r_{0.1*n}$, and the scattering of a volume distribution is $r_{0.9*V}$-$r_{0.1*V}$. When bubble radii were divided into classes of, for instance 15 μm, a number or volume distribution could be obtained in the form of a histogram. An example is presented in Figure 1. It was possible to calculate average radii, standard deviations, modes and median values, scattering intervals, and skewnesses.

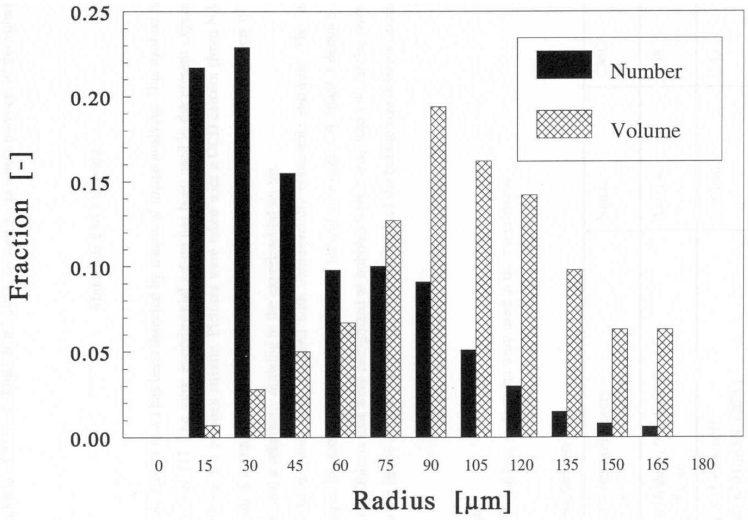


**Figure 1.** Example of distribution parameters; $r_{10}$=59.4, $\sigma_{10}$=33.9; $r_{30}$=76.5, $\sigma_{30}$=38.0; $r_{32}$=95.9, $\sigma_{32}$=49.9; $Sk_{10}$=1.030; $Sk_{30}$=-0.537; $r_{max}$=174.9; $Mo_{10}$=30-45; $Mo_{30}$=90-105; $r_{0.1*n}$=22.4, $Me_{10}$=49.4, $r_{0.9*n}$=107.3; $r_{0.1*V}$=63.3, $Me_{30}$=107.3, $r_{0.9*V}$=152.0; n=529, (all radii in μm).

In the present experimental work, the average bubble radii volume will be calculated from all experiments. To account for the distribution, the median value and a scattering interval of the median value ± 40% will be calculated from the volume distribution, as well as the skewness numbers of the volume distributions.

## Materials and Methods

The bubble size of foam has been detected by means of image analysis. This method has been described by Isarin *et al.* [1]. The same experimental set-up was used in the present experiments. The

foam flowed through a perspex cuvette. Pictures were taken with a Nikon CCD camera and recorded directly onto a PC computer . See reference [6] for a more detailed descrip tion of the experimental technique and a schematic drawing of the experi mental set-up.

The pictures were analysed with commercially obtainable software. The analysis was based upon the shape, location and dimensions of the individual images. A shape tolerance of 30% [1] was introduced. Objects that were recognised as bubbles were transposed into circles with the same average radius as the image object. These radii were the result of the bubble size determina tion.

## Materials

The following four surfactants were used in the experiments.

**Table I**. Surfactants.

| **Surfactant (manufacturer) Structure** | **Nature** | **CMC g/l** |
|---|---|---|
| Sodium Dodecyl Sulphate (Merck) $C_{12}H_{25}SO_4Na$ | anionic | 2.38 |
| Dobanol 91-8 (Shell) $C_9H_{19}(OC_2H_4)_8OH$ (20%) $C_{10}H_{21}(OC_2H_4)_8OH$ (50%) $C_{11}H_{23}(OC_2H_4)_8OH$ (30%) | non-ionic | 0.43 |
| Cetyl Trimethyl Ammonium Bromide (Fluka) $C_{16}H_{33}N(CH_3)_3Br$ | cationic | 0.335 |
| Elfan NS 242 (Akzo Nobel) $C_{12}H_{25}(OC_2H_4)_2SO_4Na$ (70%) $C_{14}H_{29}(OC_2H_4)_2SO_4Na$ (30%) | anionic | 4.135 |

CMC values were measured with a Wilhelmy plate at 25°C. All surfactants were used as received. Solutions were foamed with concentrations of 4*CMC. Pressurised air was used as the gas phase, and demineralised water was used as the solvent for the liquid phase. The surface tensions of the surfactant solutions at these concentrations were 39, 38, 34, and 31 mN/m for SDS, CTAB, Elfan, and Dobanol respectively.

To study the influence of the liquid viscosity, a thickening agent was added to a SDS solution. Solvitose C5, a natural starch from AVEBE, was used in concentrations of 0, 5, 10, 15, and 20 g/l. Liquid viscosities were measured in a rotational viscometer, and were found to be 1.3, 3.4, 8.9, 17.3, and 49.4 mPas respectively. It was assumed that the thickening agent did not influence the CMC.

Silica suspensions were foamed to study the influence of a solid phase on the bubble size distributions. The preparation of the suspen sions has been described earlier [6,20]. Cristobalite flour M5000 from Sibelco was used. Suspensions were prepared with 0, 1, 5, 10 , and 25% silica (w/w). SDS was used as the foaming agent. It was found that the silica did not influence the CMC.

## Procedure

Foam was generated in a rotor-stator mixer. The same equipment was used as described in an earlier study [6,20].

To study the effects of the rotational speed of the mixer, the viscosity of the liquid phase and the silica

content, foam was prepared with a blow ratio at an atmospheric pressure of 9 ($\Phi_{air,0}$ = 0.9). A constant liquid flow rate of 0.15 l/min was used. The tube length from the mixer to the cuvette was kept constant. The rotational speed of the mixer was varied between 400 and 2000 RPM. From each different foam, 15 pictures were taken and stored directly onto the computer. The reproducibility was studied by comparing randomly chosen pictures at 4 various rotational speeds. For the determination of the bubble size (distribution), the results of several (3-6) pictures were added up and treated as one ensemble of bubbles. The statistical parameters were calculated from these ensembles.

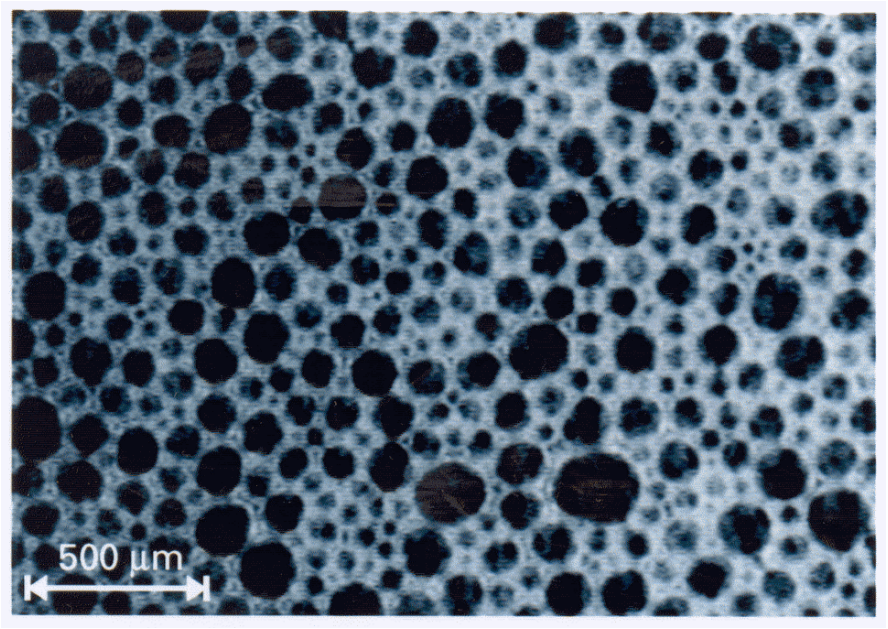


**Figure 2.** Example of fresh foam.

## Results and Discussion

The procedure of image recognising and translation to circular bubbles has been described by Isarin *et al.* [1]. Figure 2 shows a typical result of a picture of the foam obtained. The subsequent steps of image recognition and transformation to bubbles were presented earlier [1,6].

At rotational speeds of the mixer of 500, 1000, 1500, and 2000 RPM, the reproducibility of the images was studied. Volume average radii, volume scattering, volume skewness, and number skewness were calculated. The results are summarised in Figure 3. Although the results for 500 RPM are less reproducible than the results at 1000, 1500, and 2000 RPM, the reproducibility is still acceptable.

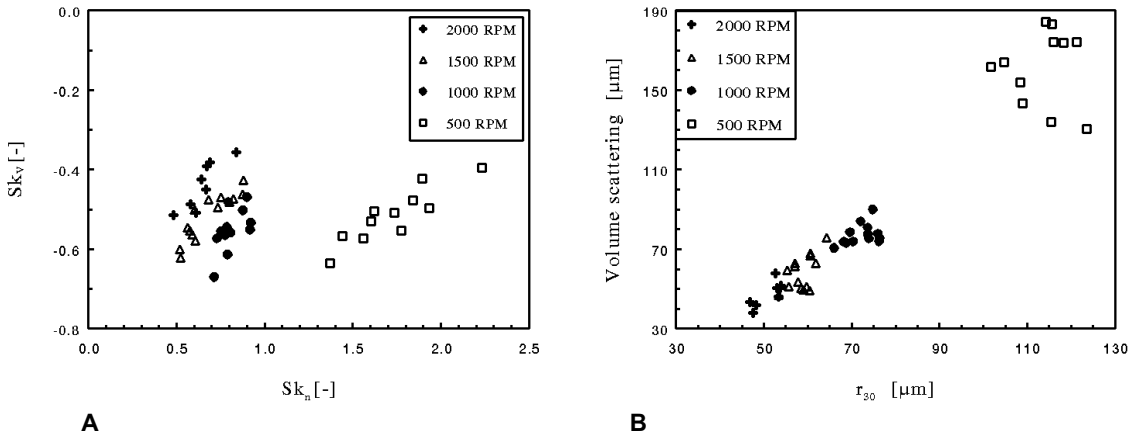


**Figure 3.** Reproducibility; A: scattering of volume distribution ($r_{0.9*V}$ - $r_{0.1*V}$) as a function of average ($r_{30}$); B: skewness of volume distribution as a function of skewness of number distribution. Results of individual pictures.

In Table 2, the results of the calculations of the most relevant statistical parameters from the ensem bles of bubbles are presented for the influence of the rotational speed with SDS as the foaming agent. These are presented graphically in Figure 4.

**Table 2.** Influence of rotational speed on bubble size and distribution.

| $N_{mix}$ (RPM) | N (-) | $r_{30}$ µm | (σ) | $r_{0.1*v}$ µm | Me µm | $r_{0.9*v}$ µm | $Sk_{30}$ | $r_{32}$ µm | (σ) |
|---|---|---|---|---|---|---|---|---|---|
| 400 | 452 | 125.1 | (90.1) | 132.8 | 241.9 | 332.6 | -0.542 | 202.6 | (151.2) |
| 500 | 509 | 111.2 | (78.2) | 118.9 | 213.8 | 299.6 | -0.504 | 178.4 | (131.0) |
| 600 | 652 | 97.8 | (63.0) | 95.5 | 169.1 | 230.5 | -0.515 | 144.4 | (97.5) |
| 750 | 685 | 80.4 | (45.8) | 70.9 | 128.4 | 186.5 | -0.472 | 109.5 | (65.8) |
| 1000 | 617 | 68.9 | (33.8) | 57.2 | 98.3 | 129.6 | -0.553 | 85.8 | (44.0) |
| 1250 | 763 | 60.6 | (26.9) | 49.7 | 82.7 | 111.2 | -0.512 | 72.8 | (33.8) |
| 1500 | 891 | 55.2 | (23.3) | 44.2 | 72.8 | 103.6 | -0.477 | 65.3 | (28.7) |
| 1750 | 961 | 52.2 | (20.5) | 41.7 | 66.6 | 91.7 | -0.486 | 60.3 | (24.6) |
| 2000 | 1105 | 47.6 | (17.1) | 37.5 | 59.7 | 79.1 | -0.427 | 53.8 | (20.1) |

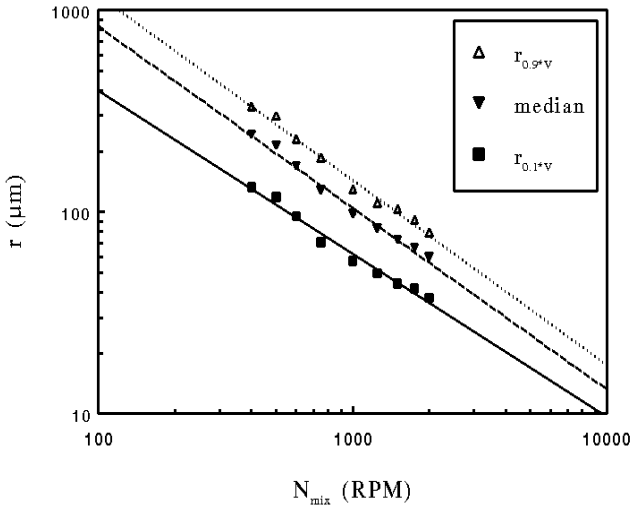


**Figure 4.** Influence of the rotational speed of the mixer on the size of the bubbles in foam; $r_{0.9*v}$, volume median and $r_{0.1*v}$

The values of the average bubble radii decrease with an increase of the rotational speed of the mixer. The average bubble radii are proportional to $(N_{mix})^{\alpha}$, with α being -0.61 for $r_{30}$. For the median values, and the under and upper limits of the scattering as presented in Figure 4, values of α were found of -0.90, -0.81, and -0.92, respectively.

Kolmogorov has pointed out that when mixing is in a turbulent regime, the size of the primary eddies is proportional to the energy input per mass to the power -0.25 [9,21,22]. If the bubble size is proportional to these primary eddies, the bubble size is proportional to the rotational speed of the mixer to the power -0.75. Others [23,24] have derived from the theory of the critical Weber number that the maximum bubble size must be proportional to the rotational speed of the mixer to the power -1.2 in the turbulent mixing regime. However, it is difficult to imagine turbulence in a foam with a dispersed phase fraction of, for instance, 0.9. The turbulence energy, as eddies, cannot be trans ported to the continuous ph ase, since the dimensions of the lamellae between the bubbles are much smaller than the size of the bubbles.

In the turbulent mixing regime, the bubble size is determined by the Weber number

$$d \propto \left( \frac{We\gamma}{\rho} \right)^{0.6} \varepsilon^{-0.4} \tag{8}$$

with ε being the energy input per unit of mass. Equation (8) finally leads to:

$$d \propto \left( \frac{\gamma}{\upsilon} \right)^{0.6} N_{mix}^{-1.2} \tag{9}$$

The bubble size is not a function of the viscosity of the liquid phase. When a constant surface tension is assumed, the bubble diameter in the turbulent regime [4]

$$d \propto \rho^{-0.6} N_{mix}^{-1.2} \tag{10}$$

In the case of mixing in the laminar regime, the bubble size is controlled by the capillary number:

$$d \propto \frac{Ca\gamma}{\eta N_{mix}} \tag{11}$$

The bubble size is not a function of the density. Again, when a constant surface tension is assumed [4]:

$$d \propto N_{mix}^{-1} \tag{12}$$

When mixing occurs in the laminar regime, the bubble size is inversely proportional to the rotational speed of the mixer [24].

Up to this point, it has been assumed that the density of the foam is constant at all rotational speeds. The bubble sizes were recorded at nearly atmospheric pressure, with a constant foam density of 100 kg/m$^3$. The pressure in the mixer was not constant at all rotational speeds , thus the foam density in the mixer was not constant. Furthermore, the bubble sizes were expanded from the mixer pressure to the atmospheric pressure. Correction for the pressure influence is easy when the ideal gas law is applied. The maximum bubble radii and the median values of the volume distributions of the four various surfactants, corrected for the mixer pressure, are shown in Figure 5. It appears that there is not much difference in the bubble radii for the various surfactants.

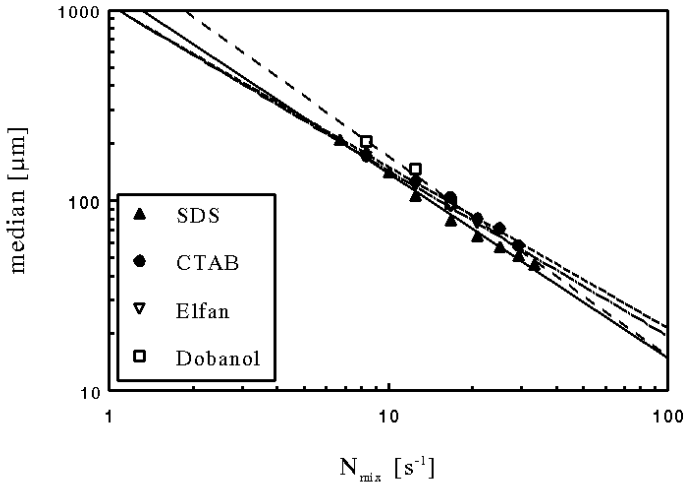


**Figure 5.** Influence of rotational speed of the mixer on the volume median values for the various foamed surfactant solutions .

Now values of α have been found of -0.97, -0.85, -0.87, and -1.05 for the median values for SDS, CTAB, Elfan, and Dobanol respectively. These values of α indicate that the mixing is in the laminar regime, although the bubble size is related to the exit of the mixer, when the foam viscosity is high. At the

entrance of the mixer, when the gas-liquid mixture has a low viscosity, turbulence could be expected. If this is correct, the viscosity of the liquid phase, or addition of silica, is expected to influence the bubble size. This is pointed out in Figures 6 and 7 for the influence of the liquid phase.

A small increase of the viscosity of the liquid phase yields a decrease of the bubble size. Above a certain viscosity there is hardly any decrease. At a high viscosity of the liquid phase and a high rotational speed, an increase of the bubble size is observed. In particular, the maximum bubble radius and the upper limit of the scattering increase. At 500 RPM, an increase of the liquid viscosity results into smaller values of all calculated radii. The skewness of the distributions is hardly influenced. At 1500 RPM, a decrease of the bubble sizes is first observed. Above a certain liquid viscosity, an increase of the large bubbles is observed; the process of bubble formation is apparently retarded. An increase of the skewnesses of the distributions is observed, due to the increase of the maximum bubble radii. At a high liquid viscosity, a stage of demixing has been reached. The skewness of the distribution with the highest liquid viscosity has been shifted from right-skewed to left-skewed. The scattering interval at 1500 RPM increases at increasing liquid viscosities, while it decreases at increasing viscosity of the liquid phase at 500 RPM.

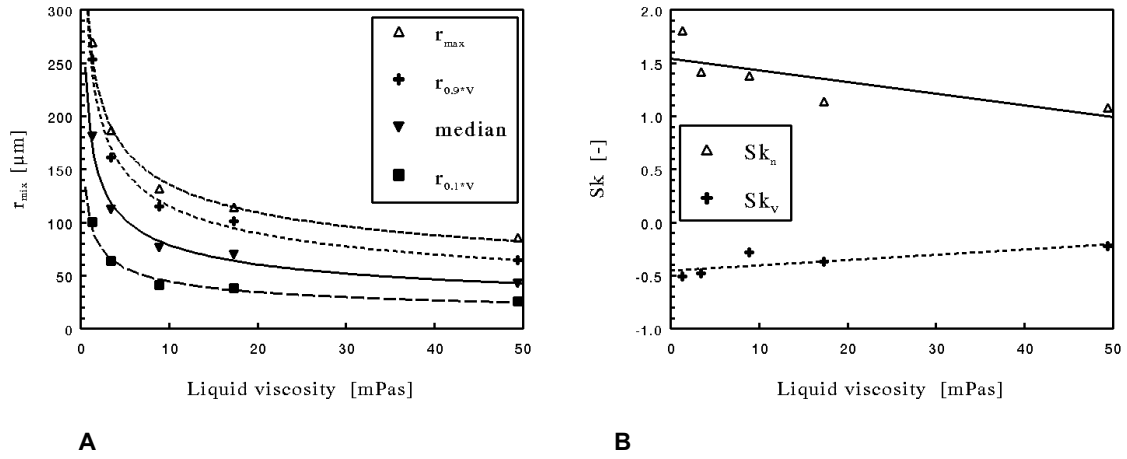


**Figure 6**. Influence of liquid viscosity on the bubble size at a rotational speed of the mixer of 500 RPM; A: maximum radii, median values, and scattering, B: skewness.

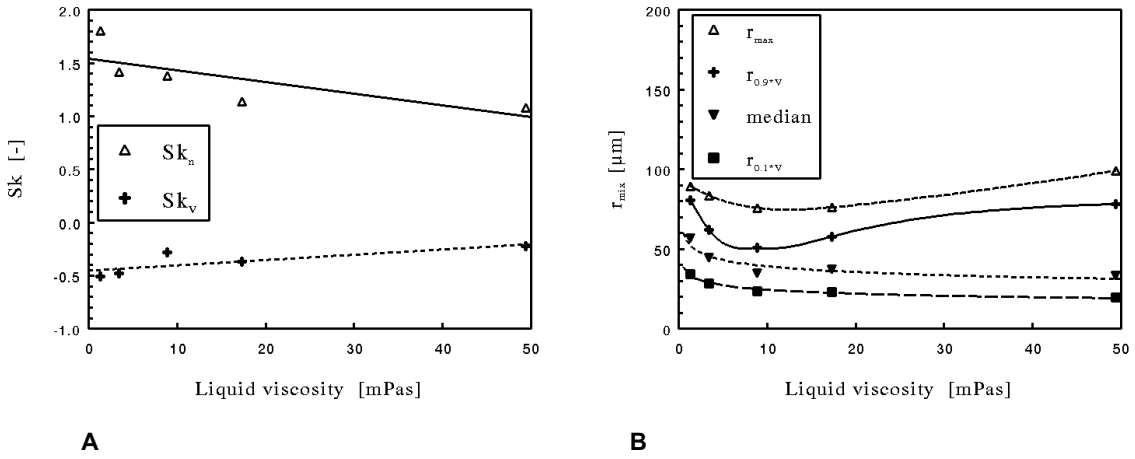


**Figure 7.** Influence of liquid viscosity on the bubble size at a rotational speed of the mixer of 1500 RPM; A: maximum radii, median values, and scattering, B: skewness.

Another explanation could be the non-Newtonian behaviour of the thickened solutions. In a first approximation, these solutions were assumed to behave as a Newtonian liquid. This was not a good assumption for solutions with a high concentration of thickening agent, which appeared to behave more like fluids which satisfy the power law [6]. Consequently, the apparent viscosity of the liquid phase may be lower in the mixer when a solution with a high concentration of thickening agent is foamed, resulting in larger bubbles.

It is found that at constant rotational speed of the mixer, the average bubble radius ($r_{30}$) is proportional to $(\eta_{liq})^{\alpha}$, with α being -0.23, -0.14, and -0.09, at 500, 1000, and 1500 RPM, respectively.

In Figure 8 and 9 the results of the bubble size determination of the three-phase foam are visualised for 500 RPM and 1500 RPM, respectively. The bubble size is hardly influenced by silica in the suspension.

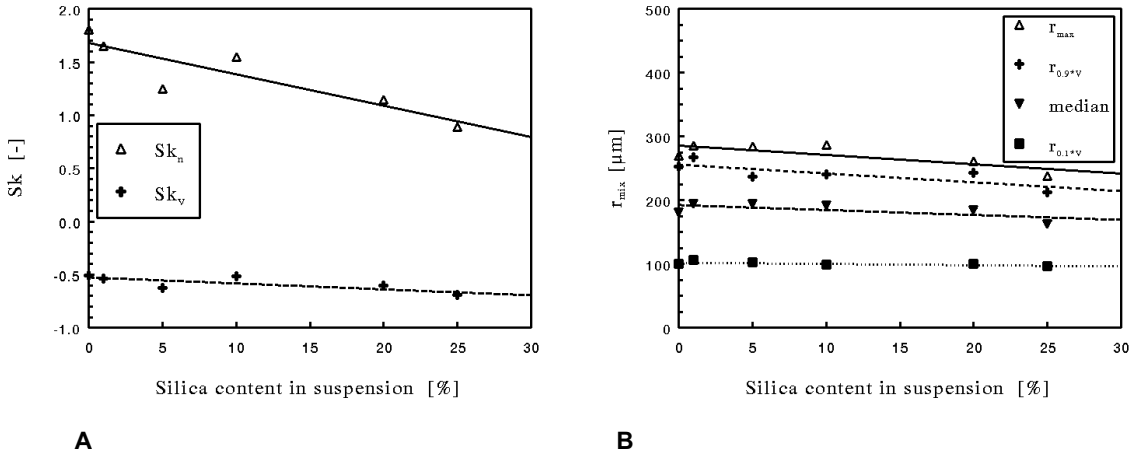


A B

**Figure 8.** Influence of silica on bubble size distribution at a rotational speed of 500 RPM; A: median values, and scattering, B: skewness.

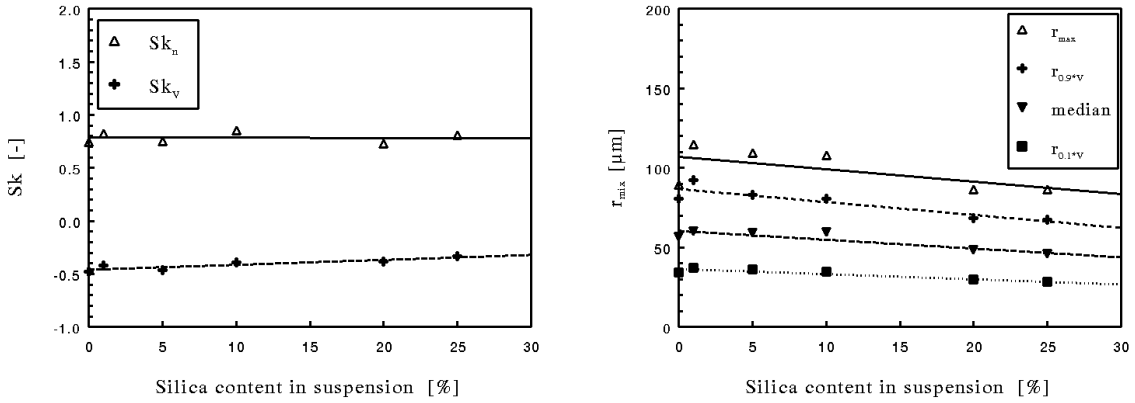


A B

**Figure 9.** Influence of silica on bubble size distribution at a rotational speed of 1500 RPM; A: median values, and scattering, B: skewness.

A small increase of the silica content results in an increase of bubble size for both rotational speeds of the mixer. A further increase of the silica content slowly decreases the bubble size. The skewness of the foam at 500 RPM decreases for the number distribution when the silica content is increased. At the rotational mixer speed of 1500 RPM, there is hardly any change in either bubble size or skewness of the distribution.

From the bubble size and the foam density, it is possible to estimate the size of the thickness of the film between the bubbles. The fraction of liquid in a foam divided by half the total surface of the bubbles in that volume of foam (since a film has two sides) gives the thickness of the film.

$$h = \frac{2}{A} \Phi_{liq} V_{foam} \tag{13}$$

If we assume a spherical shape of the bubbles, the number of bubbles can be calculated by

$$n = \frac{V_{foam}\,\Phi_{air}}{\frac{4}{3}\pi\, r_{32}^3} \tag{14}$$

The expression for the total surface of the bubbles in a volume of foam becomes

$$A = n\,4\pi\, r_{32}^2 = \frac{4\pi\, r_{32}^2}{\frac{4}{3}\pi\, r_{32}^3}\Phi_{air}\, V_{foam} = \frac{3}{r_{32}}\Phi_{air}\, V_{foam} \tag{15}$$

Introducing equation (15) into (13) yields

$$h = c\frac{2}{3} r_{32}\,\frac{\Phi_{liq}}{\Phi_{air}} = c\frac{2}{3} r_{32}\, B^{-1} \tag{16}$$

In equation (16), c is a number that corrects for the amount of liquid being held in the films and which is not in the plateau borders. If the bubble shape deviates from spheres, it is found that the surface area of one bubble is larger than a spherical bubble with the same volume [25]. In equation (16) the value for $r_{32}$ would become smaller, and the thickness of the film would thus also become smaller.

It is found that the fraction of liquid held in the films is a function of the bubble size and the foam density [26]. For bubble sizes of approximately 1000 μm and a foam density of 50 kg/m$^3$, fractions of liquid held in the films of 0.3-0.6 were found. The fractions decreased for decreasing bubble sizeor for decreasing foam density. For a blow ratio B = 9 ($\rho_{foam}$ = 100 kg/m$^3$), and the values for the bubble radius ($r_{32}$) of Table II, and assuming values of 0.3<c<0.6, it is possible to calculate the value of the thickness of the film. In Table III some typical values of the film thickness are calculated for foams generated with SDS. Since no influence on bubble size from the silica content was found, no influence on the film thickness is expected either. For the foam generated with an increasing concentration of thickening agent, a decrease of the film thickness is expected, since the bubble size decreases with an increase of the liquid viscosity.
Wenzel *et al.* [27] found values of h of 1.6-15.5 μm.

**Table 3.** Results for the film thickness

| **$N_{mix}$ (RPM)** | **h (μm)** | | |
|---|---|---|---|
| | **c=0.3** | **c=0.45** | **c=0.6** |
| 2000 | 1.2 | 1.8 | 2.4 |
| 1750 | 1.3 | 2.0 | 2.7 |
| 1500 | 1.5 | 2.2 | 2.9 |
| 1250 | 1.6 | 2.4 | 3.2 |
| 1000 | 1.9 | 2.9 | 3.8 |
| 750 | 2.4 | 3.7 | 4.9 |
| 600 | 3.2 | 4.8 | 6.4 |
| 500 | 4.0 | 5.9 | 7.9 |
| 400 | 4.5 | 6.8 | 9.0 |

The results as presented in Table 3 are for the two-phase foam. However, the bubble size of three-phase foam is of the same order of magnitude. This indicates that the film thickness is also of the same order of magnitude. The size of the silica particles was found to be up to 5 μm [6,20]. This indicates that the solid phase is mostly in the plateau borders and not in the films.

According to Cheng & Lemlich [28], there are some sources of error in the determination of the bubble size distribution when photography is involved. When pictures are taken from foam bubbles directly near a solid surface, small bubbles are excluded. Consequently, a bubble size is measured which is too large with respect to the bubble size of the foam that is further away from the solid surface. This error can be corrected mathematically when the distribution function is known:

$$F(r) = \frac{f(r)}{r}\left\{\int_0^\infty \frac{f(r)}{r}dr\right\}^{-1} \qquad (17)$$

with f(r) the measured bubble size distribution function (near the solid surface), and F(r) the corrected distribution function. It appears from equation (17) that, for instance, $r_{10}$ of the uncorrected distribution equals $r_{21}$ of the corrected distribution.

Another source of error is the fact that bubbles are distorted near a solid surface [9]. Bubbles are not completely spherical near the solid surface. The relation between the measured distorted radius and the real undistorted radius is not known, although the undistorted radius will probably be smaller than the distorted radius of a bubble near the surface.

Leonard & Lemlich [29] found that in flowing foam large bubbles were found in the centre of the flow, which were hidden by smaller bubbles near the side of the flow.

Due to interbubble gas diffusion, (rapid) disproportion is another source of error. Large bubbles grow at the expense of smaller bubbles. The bubble size distribution changes over time [6].

These four sources of error in the determination of the bubble size and distribution make it almost impossible to make any quantitative correction which takes all four sources into account. To apply equation (17) to correct the bubble size seems useless. In this investigation, no corrections whatsoever have been applied to the obtained data.

## Conclusions

Image analysis is an excellent method of determining the bubble size and its distribution in (three-phase) foam.

The bubble size decreases when the rotational speed of the mixer is increased, at constant foam density.

The proportionality of the bubble size to $(N_{mix})^{\alpha}$, with α being approximately -0.9, strongly indicates that the flow regime in the mixer is laminar. However, this is related to the exit of the foam from the mixer. At the beginning of the mixing process, when entering the mixer, mixing may be in the turbulent regime, especially when the viscosity of the gas-liquid mixture is low.

Only small influence of the nature of the surfactant on bubble size is found.

The distribution of the bubble size is represented as a scattering interval, in this study of 80% (*i.e.* a median of ± 40%).

The skewness of the volume distribution is barely affected by the rotational speed of the mixer. The skewness of the number distribution decreases for increasing rotational speeds of the mixer.

The bubble size decreases when the liquid viscosity is increased. The skewness is strongly affected by

the liquid viscosity; an increase of the viscosity results in a higher skewness number. This is the result of the increase of the maximum bubble size.

The bubble size is hardly affected by the silica content in the suspension. The skewness is hardly affected by an increase of the silica content in the suspension.

The thickness of the film is proportional to the bubble size and inversely proportional to the blow ratio. Film thicknesses were found in the range of 1-9 μm.

The bubble size distributions obtained were not subjected to any correction operation.

## *Acknowledgement*

*This research would not have been possible without the financial support of the Dutch Foundation 'Technologie van Gestructureerde Materialen'.*

**Symbols**

| | | |
|---|---|---|
| A | Surface area | $m^2$ |
| B | Blow ratio | - |
| c | Fraction of liquid in films | - |
| Ca | Capillary number | - |
| D | Diameter of the mixer | m |
| d | Diameter of a bubble | m |
| F(r) | Distribution function | - |
| f(r) | Uncorrected distribution function | - |
| h | Thickness of the film | m |
| Me | Median | m |
| Mo | Mode | m |
| $N_{mix}$ | Rotational speed of the mixer | $s^{-1}$ |
| n | Number of bubbles | - |
| R | Dimensionless radius ($r/\bar{r}$ 1) | - |
| r | Radius | m |
| $\bar{r}$ | Average bubble radius | m |
| $r_{0.1*n}$ | Under limit of 80% scattering interval of number distribution | m |
| $r_{0.9*n}$ | Upper limit of 80% scattering interval of number distribution | m |
| $r_{0.1*V}$ | Under limit of 80% scattering interval of volume distribution | m |
| $r_{0.9*V}$ | Upper limit of 80% scattering interval of volume distribution | m |
| $r_{10}$ | Number-average bubble radius | m |
| $r_{30}$ | Volume-average bubble radius | m |
| $r_{32}$ | Volume-surface-average bubble radius | m |
| Sk | Skewness number | - |
| V | Volume | $m^3$ |
| We | Weber number | - |
| y | Silica content | % |
| α | Exponential value | $N\ m^{-1}$ |
| ε | Power consumption per unit of mass | $J\ s^{-1}\ kg^{-1}$ |
| $\rho_{foam}$ | Foam density | $kg\ m^{-3}$ |
| σ | Standard deviation | m |
| η | Viscosity | Pa s |
| $\Phi_{air}$ | Volume fraction of air | - |
| $\Phi_{air,0}$ | Volume fraction of air at atmospheric pressure | - |
| $\Phi_{liq}$ | Volume fraction of liquid | - |

## *References*


1. *Isarin, J.C., Kaasjager, A.D.J., and Holweg, R.B.M., Textile Res. J., Vol 64, (1995) pp 61*
2. *Princen, H.M., J. Colloid Interface Sci., Vol 105, (1985) pp 150*
3. *Princen, H.M., and Kiss, A.D., J. Colloid Interface Sci., Vol 128, (1989) pp 176*
4. *Garrett, P.R., Chem. Eng. Sci., Vol 48, (1993) pp 367*
5. *Ranadive, A.Y., and Lemlich, R., J. Colloid Interface Sci., Vol 70, (1979) pp 392*
6. *Den Engelsen, C.W., 'Structure, Properties, and Behaviour of Three-Phase Foam', Ph-D Thesis, University of Twente, Enschede, The Netherlands, (1996)*
7. *Bisperink, C.G.J., Ronteltap, A.D., and Prins, A., Adv. Colloid Interface Sci., Vol 38, (1992) pp 13*
8. *Gido, S.P., Hirt, D.E., Montgomery, S.M., Prud'homme, R.K., and Rebenfeld, L, J. Disp. Sci. Tech., Vol 10, (1989) pp 785*
9. *Kroezen, A.B.J., 'Flow Properties of Foam in Rotor-Stator Mixers and Distribution Equipment', Ph.D. Thesis, University of Twente, Enschede, The Netherlands, (1988)*
10. *Hirt, D.E., Prud'homme, R.K., and Rebenfeld, L., J. Disp. Sci. Tech., VOL 8, (1987) pp 55*
11. *Chang, R.C., Schoen, H.M., and Grove, C.S., Ind. Eng. Chem., Vol 48, (1956) pp 2035*
12. *Calvert, J.R., and Nezhati, K., Int. J. Heat Fluid Flow, Vol 8, (1987) pp 102*
13. *Thondavadi, N.N., and Lemlich, R., Ind. Eng. Chem. Process Des. Dev., Vol 24, (1985) pp 748*
14. *De Vries, A.J., 'Foam Stability, A Fundamental Investigation of the Factors Controlling the Stability of Foams', Rubber-Stichting, Delft, The Netherlands, (1957)*
15. *Gal-Or, B., and Hoelscher, H.E., A.I.Ch.E. J., Vol 12, (1966) pp 499*
16. *Ramaswami, S., Hartland, S., and Bourne, J.R., Chem. Eng. Sci., Vol 48, (1993) pp 1709*
17. *Marion, G., Sahnoun, S., Mendiboure, B., Dicharry, C., and Lachaise, J., Progr. Colloid Polymer Sci., Vol 89, (1992) pp 145*
18. *Burford, R.L., 'Basic Statistics for Business and Economics', C.E. Merrill Publishing Company, Columbus, Ohio, (1970)*
19. *Den Engelsen, C.W., Gooijer, H., Warmoeskerken, M.M.C.G., and Groot Wassink, J., J. Coated Fabrics, Vol 27, (1997) pp 92*
20. *Den Engelsen, C.W., Gooijer, H., and Groot Wassink, J., Textile Res. J., VOL 64, (1994) pp 626*
21. *Kolmogorov, A.N., (Translated from) Dokl. Akad. Nauk. SSSR, Vol 66, (1949) pp 825*
22. *Tennekes, H., and Lumley, J.L., 'A First Course in Turbulence', The MIT Press, Cambridge, USA, (1972)*
23. *Hinze, J.O., A.I.Ch.E. J., Vol 1, (1955) pp 289*
24. *Walstra, P., Chem. Eng. Sci., Vol 48, (1993) pp 333*
25. *Princen, H.M., and Levinson, P., J. Colloid Interface Sci., Vol 120, (1987) pp 172*
26. *Cheng, H.C., and Natan, T.E., Measurement and Physical Properties of Foam, (Chapter 1 in: 'Encyclopedia of Fluid Mechanics Vol 3: Gas-Liquid Flows', ed. Cheremisinoff, N.P.), Gulf Publishing Company, Houston, (1986)*
27. *Wenzel, H.G., Brungraber, R.J., and Stelson, T.E., J. Mater., Vol 5, (1970) pp 396*
28. *Cheng, H.C., and Lemlich, R., Ind. Eng. Chem. Fundam., Vol 22, (1983) pp 105*
29. *Leonard, R.A., and Lemlich, R., A.I.Ch.E. Journal, Vol 11, (1965) pp 18*